PERGAMON

Chaos, Solitons and Fractals 16 (2003) 417–429

CHAOS
SOLITONS & FRACTALS

www.elsevier.com/locate/chaos

Phase relaxation of one-particle states in closed quantum dots

K. Held [a,b], E. Eisenberg [a,b], B.L. Altshuler [a,b,*]

[a] *Physics Department, Princeton University, Princeton, NJ 08544, USA*
[b] *NEC Research Institute, 4 Independence Way, Princeton, NJ 08540, USA*

Abstract

We develop an analytical approach to analyze the effect of dephasing of one-particle states on the magnetoconductance of closed quantum dots. This approach allows us to extract dephasing rates from experimental measurements of the magnetoconductance. The dephasing rates calculated depend on the mean level spacing and are much longer than in open quantum dots. The limited experimental data available are consistent with the theoretical prediction of diverging dephasing times in finite closed systems at sufficiently low temperatures. We also consider fluctuations of the single-electron spectrum, and observe a significant effect on the conductance distribution and magnetoconductance of closed quantum dots at experimentally relevant temperatures.

1. Introduction

The study of electron phase coherence in mesoscopic structures has attracted much interest recently. In the absence of external radiation and at low temperatures, the loss of phase coherence, or dephasing, of the quasiparticles is due to electron–electron interactions. Thus, understanding the nature of low temperatures dephasing provides us a test to our description of the many-body nature of the electrons ground state. More recently, the possibility of using quantum dots as qubits has raised an additional interest in this topic. Important in this respect is the prediction of a vanishing dephasing rate in isolated quantum dots [1].

In a clean Fermi liquid the electron–electron interaction results in dephasing of the quasiparticles. Using the Fermi golden rule, the rate can be estimated to be $\sim\epsilon^2/E_F$, where ϵ is the quasiparticle energy and E_F is the Fermi energy. The effect of disorder can be incorporated, and leads to a decrease of the dephasing rate. However, when the mean level spacing, Δ, becomes large, the Fermi golden rule approach breaks down, as the density of states becomes too low (compared to the average matrix element). It was shown that the golden rule estimates are valid only for $\epsilon > \Delta\sqrt{g_T}$, where g_T is the dimensionless Thouless conductance of the system. At much lower energies, where the typical matrix elements are much smaller than Δ, the quasiparticle states do not decay, they are just slightly perturbed by the electron–electron interaction. Using a mapping onto a localization model, it was shown that there is a sharp transition between these two limits, as a result of localization of the wave-function in Fock space. Thus, one expects to find the dephasing rate to vanish at some finite temperature, which scales like [1] $\Delta\sqrt{g_T/\ln g_T}$. As mentioned above, this result, namely the possibility of a vanishing dephasing rate at finite temperatures, is of great importance to the quantum computing community. However, it was claimed that the logarithmic correction, and maybe even the existence of the transition are artifacts of various approximations done in the process of mapping the many-body Hamiltonian onto the localization problem [2]. Thus, an experimental verification of this localization transition, through measurements of the dephasing rate in closed (i.e., nearly isolated) quantum dots, is desirable.

* Corresponding author. Address: NEC Research Institute, 4 Independence Way, Princeton, NJ 08540, USA. Tel.: +1-609-951-2620; fax: +1-609-951-2496.
E-mail address: bla@research.nj.nec.com (B.L. Altshuler).

0960-0779/03/$ - see front matter
PII: S0960-0779(02)00303-X

Quantum dots which contain a larger number of electrons $\mathcal{N}$, $\mathcal{O}(10^3)$ or more, are usually described statistically. In particular, the low-energy universal statistical fluctuations of diffusive quantum dots or quantum dots with irregular shapes whose associated classical dynamics are chaotic can be described by random matrix theory (RMT), which becomes exact in the limit $1/g_T \to 0$ ($g_T \propto \sqrt{\mathcal{N}}$). Within the RMT approach, the one-particle eigenvectors as well as the dot–lead coupling are statistically distributed whereas the Coulomb interaction is independent of the levels involved. Thus, to leading order in $1/g_T$, the charging term (Coulomb repulsion) and the exchange interaction depend only on the total charge and spin, respectively [3,4]. The solution of the RMT model by means of the master or rate equation successfully described the mesoscopic fluctuations of the Coulomb blockade peaks in closed quantum dots, i.e., the statistical distribution of their height $P(G^{\max})$ and its dependence upon magnetic field [5]. On the other hand, recent experiments unambiguously show deviations from this RMT prediction, suggesting that interaction effects beyond charging should be considered as well. In particular, dephasing of the one-particle states due to interactions modifies the conductance peak height statistics (see [3,4] and references therein). Whereas there is a number of ways to measure the dephasing times in open quantum dots [6,7], the situation is much more complicated in closed dots.

Only a few experiments have attempted to study dephasing in closed quantum dots. Most of these have focused on the relaxation of highly excited states [8], verifying the continuous to discrete spectrum transition at $\epsilon \propto g\Delta$. Some signatures of dephasing in thermalized states have been studied by Patel et al. [9], who analyzed the statistical distribution of the conductance maxima $G^{\max}$ (the height of the Coulomb blockade peaks). They found that the ratio of standard deviation to mean peak height $\sigma(G^{\max})/\langle G^{\max}\rangle$ is smaller than what RMT predicts [10], and attributed this reduction to dephasing effects. More recently, Folk et al. [11] suggested to use the dependence of the conductance upon applying a magnetic field B,

$$\alpha = \frac{\langle G^{\max}\rangle_{B\neq 0} - \langle G^{\max}\rangle_{B=0}}{\langle G^{\max}\rangle_{B\neq 0}}, \tag{1}$$

as a probe of the dephasing. This is the closed dot analog of the weak localization magnetoconductance which was analyzed earlier for open dots [6]. Folk et al. found considerable deviations of α from 1/4 which is considered to be an indication for dephasing or inelastic scattering. In a first theoretical work, Beenakker et al. [12] considered the limit of strong inelastic scattering, i.e., the limit where the inelastic relaxation rate Γ_{in} far exceeds the mean tunneling rate or inverse dwell time in the dot $\overline{\Gamma}$. In this limit, α is reduced much stronger than what was found experimentally. Thus, Beenakker et al. [12] concluded that $\Gamma_{\text{in}} < \overline{\Gamma}$ in the experiment [11]. More recently, Rupp et al. [13] studied the ratio of standard deviations

$$\gamma = \frac{\sigma(G^{\max})_{B\neq 0} - \sigma(G^{\max})_{B=0}}{\sigma(G^{\max})_{B\neq 0}} \tag{2}$$

in the limit of strong inelastic scattering and suggested to use this quantity as an indicator for dephasing.

We discuss here in detail two effects that lead to a suppression of α below 1/4: While phase-breaking inelastic scattering processes can lead to the large suppression of α observed experimentally at high temperature [14], RMT fluctuations of the one-particle eigenfunctions lead to a non-negligible effect at lower temperatures [15].

The paper is organized as follows. In Section 2, we extend the master equation approach of Beenakker [16] to take into account phase-breaking inelastic scattering. In Section 3, we develop an analytical approach which is valid at high temperatures and allows us to evaluate α (Eq. (1)). This analytical approach is validated by comparing to the numerical solution. In Section 4, the closed-dot dephasing times extracted from the experimental values of α [11] are presented: We observe a clear enhancement of the dephasing times relative to earlier results for open quantum dots [6]. Moreover, contrary to the analysis of open quantum dots [6] which showed a dependence on temperature alone, we find a dependence on *both* T and Δ, not inconsistent with vanishing dephasing rates for low excitation energies [1]. Finally, in Section 5 the effect of RMT eigenlevel fluctuations on α is discussed.

2. Model

Within the RMT approach, the one-particle eigenlevels of the quantum dot E_i are Wigner-Dyson distributed, depending on the absence or presence of a magnetic field in the Gaussian orthogonal (GOE) or unitary ensemble (GUE), respectively. As we are interested in the Coulomb blockade regime, the number of electrons in the quantum dot is restricted to N and $N+1$. The Coulomb interaction is described by a constant charging energy which is different for N and $N+1$ electrons. Each state of the quantum dot is, thus, determined by a tuple $\{n_i\}$ of occupation numbers for the one-particle eigenstates with energies E_i and spins S_i. Neglecting higher order processes in the tunneling rates, the

probability $P_{\mathcal{N}}(\{n_i\})$ to find the tuple $\{n_i\}$ with $\mathcal{N} \in \{N, N+1\}$ electron can be described by the following master equation which includes the tunneling rate between dot and lead [16] as well as inelastic scattering processes

$$\frac{\mathrm{d}P_N(\{n_i\})}{\mathrm{d}t} = \sum_{j\lambda} \delta_{n_j 0} \Gamma_j^{\lambda} [(1 - f_j^{\lambda}) P_{N+1}(\{n_i\}_{+j}) - f_j^{\lambda} P_N(\{n_i\})] + \sum_{jk} \delta_{n_j 0} \delta_{n_k 1} \left[\Gamma_{\mathrm{in}}^{jk} P_N(\{n_i\}_{+j-k}) - \Gamma_{\mathrm{in}}^{kj} P_N(\{n_i\}) \right],$$

$$\frac{\mathrm{d}P_{N+1}(\{n_i\})}{\mathrm{d}t} = \sum_{j\lambda} \delta_{n_j 1} \Gamma_j^{\lambda} [f_j^{\lambda} P_N(\{n_i\}_{-j}) - (1 - f_j^{\lambda}) P_{N+1}(\{n_i\})] + \sum_{jk} \delta_{n_j 1} \delta_{n_k 0} \left[\Gamma_{\mathrm{in}}^{kj} P_{N+1}(\{n_i\}_{-j+k}) - \Gamma_{\mathrm{in}}^{jk} P_{N+1}(\{n_i\}) \right]. \tag{3}$$

Here, $\{n_i\}_{+j}$ ($\{n_i\}_{-j}$) are the tuples obtained from $\{n_i\}$ by adding (removing) one electron in the one-particle eigenstate j. The leads are thermalized and distributed according to the Fermi function $f_j^{\lambda} = f_{\mathrm{FD}}(E_j + (\delta_{\lambda L} - 1/2)eV - \mu)$, where $\lambda \in \{L, R\}$, V denote the applied voltage, and μ is the effective chemical potential, including the charging energy. The first terms in (3) describe the tunneling of electrons between the dot eigenlevels j and the two leads with rates Γ_j^{λ}. Within RMT, the distribution of these rates is given by the Porter-Thomas distribution

$$P_{\beta}(\Gamma) = \left(\frac{\Gamma}{2\langle \Gamma \rangle} \right)^{\beta/2-1} \frac{\langle \Gamma \rangle^{\beta/2-1}}{\mathcal{G}(\beta/2)} \exp[-\beta\Gamma/(2\langle \Gamma \rangle)]. \tag{4}$$

Here, $\langle \Gamma \rangle$ is the mean-value of the distribution and $\mathcal{G}$ the Gamma function. The difference between $P_1(r)$ and $P_2(r)$ leads to the afore mentioned value $\alpha = 1/4$ in the absence of inelastic scattering [17]. The inelastic scattering from a level j to another level k with rate $\Gamma_{\mathrm{in}}^{jk}$ is described by the last terms of Eq. (3). The analytic approximation which we develop in Section 3.2 depends only on the total inelastic scattering rate Γ_{in}, and therefore the details of the inelastic scattering model are not important. For the purpose of the numerical calculations to follow, we assume the following model for the scattering rates ($\omega_{jk} = E_k - E_j$)

$$\Gamma_{\mathrm{in}}^{jk} = \Gamma_{\mathrm{in}}^{0} \frac{\mathrm{sgn}(\omega_{jk}) D(|\omega_{jk}|)}{\exp[\omega_{jk}/(k_{\mathrm{B}}T)] - 1} \delta_{S_j S_k}. \tag{5}$$

This inelastic scattering rate can be caused by thermal bosonic fluctuations at temperature T with density of states $D(E)$. But it is even more general, it only assumes detailed balance, no back-coupling of the scattering to the Bose bath, and spin-independence. The microscopic mechanism might be due to external noise, electron–electron, or electron–phonon interaction. An important point w.r.t. Eq. (5) is that the suppression of α is quite robust to the specific model of interaction, and depends mainly on the *total inelastic scattering rate* Γ_{in}, as will be shown below. We consider Γ_{in} as a free (phenomenological) parameter which can be determined from the experiment.

From the stationary solution of the master equation (3), i.e., $\mathrm{d}P_{\mathcal{N}}(\{n_i\})/\mathrm{d}t = 0$, the current I can be calculated via the tunneling processes between left lead and dot

$$I = -e \sum_{\{n_i\}} \sum_{j} \delta_{n_j 0} \Gamma_j^{\mathrm{L}} [f_j P_N(\{n_i\}) - (1 - f_j) P_{N+1}(\{n_i\}_{+j})] \tag{6}$$

and from I the conductance $G = \mathrm{d}I/\mathrm{d}V$.

3. Analytical approaches

To calculate the conductance, we linearize the master equation w.r.t. the applied potential V, i.e., $f_j^{\lambda} = f_j + (\delta_{\lambda L} - \frac{1}{2})eV\,\mathrm{d}f_j/\mathrm{d}E_j$, and expand $P_{\mathcal{N}}(\{n_i\})$ up to first order in the voltage

$$P_{\mathcal{N}}(\{n_i\}) = P_{\mathcal{N}}^{\mathrm{eq}}(\{n_i\}) \left(1 + \frac{\mathrm{eV}}{k_{\mathrm{B}}T} \Psi_{\mathcal{N}}(\{n_i\}) \right) \tag{7}$$

with the equilibrium distribution

$$P_{\mathcal{N}}^{\mathrm{eq}}(\{n_i\}) \propto \mathrm{e}^{-\beta \sum_j \delta_{n_j 1}(E_j - \mu)}. \tag{8}$$

This ansatz solves the stationary master equation to order $(eV/k_{\mathrm{B}}T)^0$ because the $V = 0$ solution is the equilibrium distribution. To order $(eV/k_{\mathrm{B}}T)^1$ the stationary master equation (3) corresponds to the following equation for $\Psi_{\mathcal{N}}(\{n_i\})$,

$$
\begin{aligned}
0 &= \sum_j \delta_{n_j 0}\Bigg\{\left(\Gamma_j^{\mathrm{L}}+\Gamma_j^{\mathrm{R}}\right) f_j[\Psi_{N+1}(\{n_i\}_{+j})-\Psi_N(\{n_i\})]+\frac{\Gamma_j^{\mathrm{L}}-\Gamma_j^{\mathrm{R}}}{2}f_j \\
&\qquad +\sum_k \delta_{n_k 1}\Gamma_{\mathrm{in}}^{kj}[\Psi_{\mathscr{N}}(\{n_i\}_{+j-k})-\Psi_{\mathscr{N}}(\{n_i\})]\Bigg\}, \\
0 &= \sum_j \delta_{n_j 1}\Bigg\{\left(\Gamma_j^{\mathrm{L}}+\Gamma_j^{\mathrm{R}}\right)(1-f_j)[\Psi_N(\{n_i\}_{-j})-\Psi_{N+1}(\{n_i\})]-\frac{\Gamma_j^{\mathrm{L}}-\Gamma_j^{\mathrm{R}}}{2}(1-f_j) \\
&\qquad -\sum_k \delta_{n_k 0}\Gamma_{\mathrm{in}}^{jk}[\Psi_{\mathscr{N}+1}(\{n_i\})-\Psi_{\mathscr{N}+1}(\{n_i\}_{-j+k})]\Bigg\}.
\end{aligned}
\tag{9}
$$

To arrive at (9), we use the following relations:

$$
\begin{aligned}
&P_{N+1}^{\mathrm{eq}}(\{n_i\}_{+j})/P_N^{\mathrm{eq}}(\{n_i\}) = \mathrm{e}^{-\beta(E_j-\mu)} = \frac{f_j}{1-f_j}, \\
&\Gamma_{\mathrm{in}}^{jk}/\Gamma_{\mathrm{in}}^{kj} = \mathrm{e}^{-\beta[E_k-E_j]}, \\
&\mathrm{d}f_j/\mathrm{d}E_j = -\beta f_j(1-f_j).
\end{aligned}
$$

3.1. Perturbation theory in $\overline{\Gamma}/\Gamma_{\mathrm{in}}$

In the limit of large inelastic scattering $\overline{\Gamma}/\Gamma_{\mathrm{in}} \to 0$ ($\overline{\Gamma}=\overline{\Gamma}^{\mathrm{L}}+\overline{\Gamma}^{\mathrm{R}}$ denotes the inverse dwell time and $\overline{\Gamma}^{\lambda}$ the mean tunneling rate to lead λ), the inelastic scattering term dominates the master equations (9) and equilibrates all levels with $\mathscr{N}=N$ electrons with each other. The same holds for $\mathscr{N}=N+1$ but levels with different $\mathscr{N}$ are not equilibrated. Thus,

$$
\Psi_{\mathscr{N}}(\{n_i\}) = \Psi_{\mathscr{N}} \tag{10}
$$

becomes independent of $\{n_i\}$. In this case one has to solve a master equation for $\Psi_{\mathscr{N}}$ which results in [16]

$$
\Psi_{\mathscr{N}} = \mathrm{const} + \frac{1}{2}\frac{\langle\!\langle \Gamma^{\mathrm{R}}-\Gamma^{\mathrm{L}}\rangle\!\rangle}{\langle\!\langle \Gamma^{\mathrm{R}}+\Gamma^{\mathrm{L}}\rangle\!\rangle}\delta_{\mathscr{N}N+1}, \tag{11}
$$

where

$$
\langle\!\langle X\rangle\!\rangle = \sum_j [1-F_{\mathrm{eq}}(E_j|N)]f_j X_j. \tag{12}
$$

Here, $F_{\mathrm{eq}}(E_j|N)$ is the equilibrium probability to have level E_j occupied if N electrons are in the quantum dot. At high temperatures $F_{\mathrm{eq}}(E_j|N)$ can be replaced by the Fermi distribution f_j.

In a first step beyond the infinite inelastic scattering limit, we apply perturbation theory in $\overline{\Gamma}/\Gamma_{\mathrm{in}}$. We employ the ansatz

$$
\Psi_{\mathscr{N}}(\{n_i\}) = \Psi_{\mathscr{N}} + \frac{\overline{\Gamma}}{\Gamma_{\mathrm{in}}^{*}}\sum_j \delta_{n_j 1}\delta\Psi(j), \tag{13}
$$

where $\Gamma_{\mathrm{in}}^{*}=\Gamma_{\mathrm{in}}^{j}/(1-f_j)$ depends only weakly on j for the levels around the Fermi energy which contribute to the conductance and $\Gamma_{\mathrm{in}}^{j}=\sum_k[1-F_{\mathrm{eq}}(E_k|\mathscr{N})]\Gamma_{\mathrm{in}}^{jk}$ is the inelastic scattering rate for level j (we refer to Γ_{in} as Γ_{in}^{j} for $E_j=0$). With the ansatz (13), the second equation of (9) reads to leading order in $\overline{\Gamma}/\Gamma_{\mathrm{in}}$:

$$
0 = \sum_j \delta_{n_j 1}\Bigg\{(\Gamma_j^{\mathrm{L}}+\Gamma_j^{\mathrm{R}})(1-f_j)\frac{1}{2}\frac{\langle\!\langle \Gamma^{\mathrm{R}}-\Gamma^{\mathrm{L}}\rangle\!\rangle}{\langle\!\langle \Gamma^{\mathrm{R}}+\Gamma^{\mathrm{L}}\rangle\!\rangle}+\frac{\Gamma_j^{\mathrm{L}}-\Gamma_j^{\mathrm{R}}}{2}(1-f_j)+\sum_k \delta_{n_k 0}\Gamma_{\mathrm{in}}^{jk}\frac{\overline{\Gamma}}{\Gamma_{\mathrm{in}}^{*}}[\delta\Psi(j)-\delta\Psi(k)]\Bigg\}. \tag{14}
$$

Every addend j of this sum vanishes for the solution

$$
\delta\Psi(j) = -\frac{1}{2}\frac{\langle\!\langle \Gamma^{\mathrm{R}}-\Gamma^{\mathrm{L}}\rangle\!\rangle}{\langle\!\langle \Gamma^{\mathrm{R}}+\Gamma^{\mathrm{L}}\rangle\!\rangle}\frac{\Gamma_j^{\mathrm{L}}+\Gamma_j^{\mathrm{R}}}{\overline{\Gamma}}-\frac{1}{2}\frac{\Gamma_j^{\mathrm{L}}-\Gamma_j^{\mathrm{R}}}{\overline{\Gamma}}. \tag{15}
$$

Eq. (15) also solves the first master Eq. (9) if one takes into account that $\Gamma_{\rm in}^{jk}/\Gamma_{\rm in}^{kj} = (1-f_j)/f_j f_k/(1-f_k)$. Thus, the ansatz solves the stationary master Eq. (9). Note that since the average of $\delta\Psi(j)$ is zero, the term $\sum_k \Gamma_{\rm in}^{jk}\delta\Psi(k)$, which averages over many levels k, is zero in the leading order in $\Delta/(k_{\rm B}T)$.

The solution (15) of the master equation yields the conductance

$$G = \frac{e^2}{k_{\rm B}T} P^{\rm eq}(N)\left(\frac{\langle\!\langle \Gamma^{\rm L}\rangle\!\rangle\langle\!\langle \Gamma^{\rm R}\rangle\!\rangle}{\langle\!\langle \Gamma^{\rm L}+\Gamma^{\rm R}\rangle\!\rangle} - \frac{\langle\!\langle \Gamma^{\rm L^2}\rangle\!\rangle\langle\!\langle \Gamma^{\rm R}\rangle\!\rangle^2 + \langle\!\langle \Gamma^{\rm R^2}\rangle\!\rangle\langle\!\langle \Gamma^{\rm L}\rangle\!\rangle^2 - 2\langle\!\langle \Gamma^{\rm L}\rangle\!\rangle^2\langle\!\langle \Gamma^{\rm R}\rangle\!\rangle^2}{\Gamma_{\rm in}^{*}\langle\!\langle \Gamma^{\rm L}+\Gamma^{\rm R}\rangle\!\rangle^2}\right), \tag{16}$$

$$\alpha = \frac{1}{12}\frac{\Delta}{k_{\rm B}T} + \frac{\overline{\Gamma}}{2\Gamma_{\rm in}}, \tag{17}$$

where $P^{\rm eq}(N)$ is the equilibrium probability to have N electrons in the dot. This result reproduces the limit $\overline{\Gamma}/\Gamma_{\rm in} \to 0$ of [16] and holds to first order in $\overline{\Gamma}/\Gamma_{\rm in}$ and $\Delta/k_{\rm B}T$. In particular, it describes correctly the high temperatures regime, since for a typical scattering model $\overline{\Gamma}/\Gamma_{\rm in} \to 0$ for $\Delta/k_{\rm B}T \to 0$.

3.2. Approximative analytical solution

The inelastic scattering model (5) is exponentially cut off to states outside an energy window of $\mathcal{O}(k_{\rm B}T)$ and, thus, $\Gamma_{\rm in}$ vanishes at low temperatures. At $k_{\rm B}T \gg \Delta$, on the other hand, there are many states $M \propto T/\Delta$ connected by the inelastic scattering. Therefore, for $T \to \infty$, the total inelastic scattering rate $\Gamma_{\rm in}/\overline{\Gamma} \to \infty$ and the result (17) is approached. Inspired by the high-temperature perturbative expansion, we develop in the following a self-consistent approximation. Similar to (13), we employ the ansatz

$$\Psi_{\mathcal{N}}(\{n_i\}) = \sum_j \delta_{n_j 1}\Psi(j). \tag{18}$$

With this ansatz, the master equation (9) reads for every addend j:

$$\begin{aligned} 0 &= (\Gamma_j^{\rm L}+\Gamma_j^{\rm R})f_j\Psi(j) + (\Gamma_j^{\rm L}-\Gamma_j^{\rm R})f_j/2 - \sum_k \delta_{n_k 1}\Gamma_{\rm in}^{kj}[\Psi(k)-\Psi(j)], \\ 0 &= -(\Gamma_j^{\rm L}+\Gamma_j^{\rm R})(1-f_j)\Psi(j) - (\Gamma_j^{\rm L}-\Gamma_j^{\rm R})(1-f_j)/2 + \sum_k \delta_{n_k 0}\Gamma_{\rm in}^{jk}[\Psi(k)-\Psi(j)]. \end{aligned} \tag{19}$$

With a large number of final states to scatter to, we can decouple the scattering amplitudes $\delta_{n_k 0}\Gamma_{\rm in}^{jk}$ and occupations $\Psi(k)$ in Eq. (19)

$$\sum_k \delta_{n_k 0}\Gamma_{\rm in}^{jk}\Psi(k) \to \underbrace{\sum_k \delta_{n_k 0}\Gamma_{\rm in}^{jk}}_{\Gamma_{\rm in}^{j}}\overline{\Psi}. \tag{20}$$

Here, $\overline{\Psi}$ should, in principle, be a weighted average over levels within a range of $\mathcal{O}(k_{\rm B}T)$ around a particular level j considered. However, only levels around the Fermi energy are of interest for the conductance since the contribution of every level j to the conductance is multiplied by $f_j(1-f_j)$. For this reason, we approximately treat

$$\overline{\Psi} = \sum_j f_j(1-f_j)\Psi(j)\Big/\left(\sum_j f_j(1-f_j)\right) \tag{21}$$

in Eqs. (19) and (20) as a constant, and neglect the j dependence of $\Gamma_{\rm in}^{*}$. With this approximation, the solution for both Eqs. (19) is

$$\Psi(j) = \frac{(\Gamma_j^{\rm R}-\Gamma_j^{\rm L})/2 + \Gamma_{\rm in}^{*}\overline{\Psi}}{\Gamma_{\rm in}^{*}+\Gamma_j^{\rm L}+\Gamma_j^{\rm R}}, \tag{22}$$

where self-consistency yields

$$\overline{\Psi} = \frac{1}{2}\frac{\langle\!\langle (\Gamma^{\rm R}-\Gamma^{\rm L})\tau^{\rm tot}\rangle\!\rangle}{\langle\!\langle (\Gamma^{\rm R}+\Gamma^{\rm L})\tau^{\rm tot}\rangle\!\rangle} \tag{23}$$

with $\tau_i^{\rm tot} = (\Gamma_i^{\rm L}+\Gamma_i^{\rm R}+\Gamma_{\rm in}^{*})^{-1}$. Since the ansatz (18) solves the master equation (9) it is a posteriori justified to use this ansatz. From the approximate solution (22), one obtains the conductance

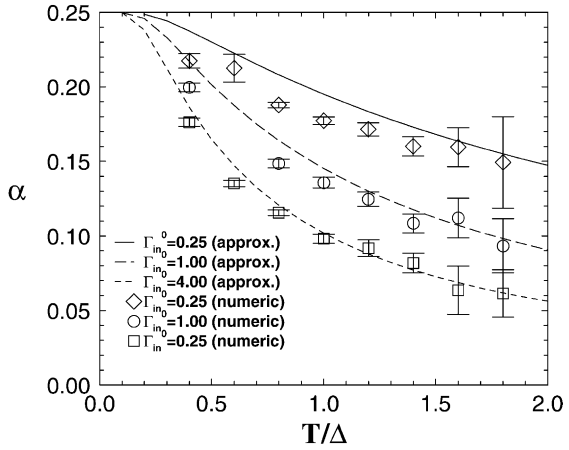

Fig. 1. Comparison of the numerical solution of the full master equation with the high temperature approximation. The latter is seen to work well for $k_B T > \Delta$ (reproduced from [14]).

$$G = \frac{e^2}{k_B T} P^{\mathrm{eq}}(N) \left\langle \left\langle \Gamma_i^{\mathrm{L}} \tau_i^{\mathrm{tot}} \left(\Gamma_i^{\mathrm{R}} + \frac{\Gamma_{\mathrm{in}}^{*} \langle\langle \Gamma_j^{\mathrm{R}} \tau_j^{\mathrm{tot}} \rangle\rangle}{\langle\langle (\Gamma_j^{\mathrm{L}} + \Gamma_j^{\mathrm{R}}) \tau_j^{\mathrm{tot}} \rangle\rangle} \right) \right\rangle \right\rangle. \tag{24}$$

One would obtain the same form (24) but with $\langle\langle \cdots \rangle\rangle = \sum_{j=1}^{M} \cdots$ considering M degenerate levels filled with $N \in \{0, 1\}$ electrons.

The result (24) can be interpreted in the following way: the first term represents processes in which the electron was not scattered at all. These happen with probability $(\Gamma_i^{\mathrm{L}} + \Gamma_i^{\mathrm{R}})\tau_i^{\mathrm{tot}}$ and the resulting conductance peak heights are proportional to $\Gamma_i^{\mathrm{L}}\Gamma_i^{\mathrm{R}}/(\Gamma_i^{\mathrm{L}} + \Gamma_i^{\mathrm{R}})$; yielding $\Gamma_i^{\mathrm{L}}\Gamma_i^{\mathrm{R}}\tau_i^{\mathrm{tot}}$ altogether. The second term represents contributions from electrons that were inelastically scattered after tunneling from one lead, and their contribution to the conductance is $\langle\langle \Gamma_j^{\mathrm{R}} \tau_j^{\mathrm{tot}} \rangle\rangle / \langle\langle (\Gamma_j^{\mathrm{L}} + \Gamma_j^{\mathrm{R}}) \tau_j^{\mathrm{tot}} \rangle\rangle$.

Eq. (24) is the main result of this section. It is based on approximation (20) which can be justified in the high temperature limit. The particular advantage of this approach is that it gives not only the correct leading high temperature behavior (Eq. (16)) but also reproduces correctly the limits $\Gamma_{\mathrm{in}} = 0$ and $\Gamma_{\mathrm{in}} = \infty$ for all T including $\alpha = 1/4$ at $T = 0$. Below we demonstrate that this approach works pretty well in the regime $k_B T \sim \Delta$.

In order to calculate G and α one has to average Eq. (24) w.r.t. the different ensembles. One could do so numerically, but it is possible to get analytical results via expanding Eq. (24) in powers of $\Delta/k_B T$. This procedure is described in detail in the appendix. In the following we use the results of this expansion as our estimate of the dephasing rate.

3.3. Numerical and experimental tests

To test the validity of the approximative analytical solution, we compare the results to the numerical solution. The latter is obtained by solving the master equation (3) by sparse matrix inversion. [1] As we are interested in not too low temperatures, we assume in the following a picket-fence distribution of the one-particle eigenlevels with spacing Δ between consecutive spin-degenerate levels ($E_{2j} = E_{2j-1} = j\Delta$; $\Gamma_{2j}^{\lambda} = \Gamma_{2j-1}^{\lambda}$; $\overline{\Gamma}_j^{\lambda} = \overline{\Gamma}/2$).

Fig. 1 compares values of the analytical approximation for α with the numerical values. The agreement is very good for sufficiently high temperatures, and reasonable even for low T. In the whole temperature regime, the deviations are within current experimental accuracy of magnetoconductance measurements. Fig. 1, thus, shows that the analytical approach provides a reliable way to determine Γ_{in} from experimental measurements of α, in the whole temperature regime.

Due to the phenomenological nature of our approach with a free parameter Γ_{in} (i.e., unspecified dephasing mechanism), we cannot *predict* the dephasing rate of a given sample. However, a direct experimental test is provided by measuring values of α in a given dot at *fixed* T, as a function of $\overline{\Gamma}$ (which can be achieved by changing the contact

[1] For $k_B T < 1.6\Delta$, we took into account all configurations $\{n_i\}$ which involve levels in $[-4k_B T \cdots 4k_B T]$ with $P^{\mathrm{eq}}\{n_i\}/\min_{\{n_i\}} P^{\mathrm{eq}}\{n_i\} > \exp(-5\Delta/k_B T)$; for $k_B T > 1.6\Delta$ the interval was $[-3k_B T \cdots 3k_B T]$ and the exponential cut-off $-4.5\Delta/k_B T$.

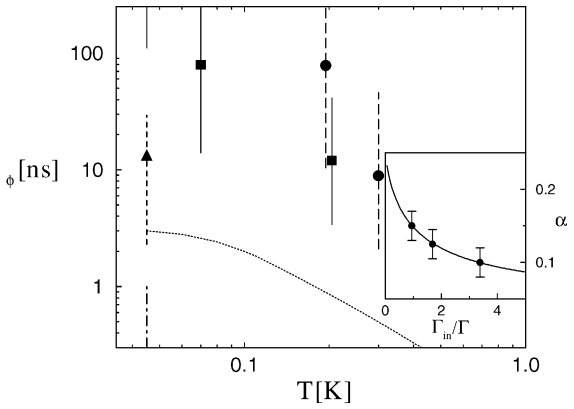

Fig. 2. Dephasing times, τ_ϕ, as extracted from the data points in [11] for four different dots: $\Delta = 28$ μeV (circles, long-dashes error bars), $\Delta = 10$ μeV (squares, solid error bars), $\Delta = 2.4$ μeV (up-triangles, dashed error bar), and $\Delta = 0.9$ μeV (dot-dashed error bar); dotted line: fit so open dot experiments as calculated in [6]. Error bars which extend up (down) beyond the graph should be understood as going up to infinity (down to zero); if no corresponding point is visible the experimental mean value itself gives $\tau_\phi = \infty$ (or $\tau_\phi = 0$). In the inset, we fit experimental measurements for different values of $\overline{\Gamma}$ [11] with our theory. The single fitting parameter is $\Gamma_{in} = 0.25$ μeV, or $\tau_\phi = 16$ ns (reproduced from [14]).

setting). The theoretical dependence of α on $\overline{\Gamma}$ involves a single fitting parameter, i.e., the unknown total scattering rate Γ_{in} which is assumed to be unaffected by the contact setting. A first step in this direction was done in [11], and in the inset of Fig. 2 we compare the prediction of our high temperature approximation with the measurements of α for three different values of $\overline{\Gamma}$. An excellent agreement is obtained, though more data points are required for reliable conclusions.

4. Results

The good agreement of our approach with numerical solutions, together with the excellent agreement with the limited experimental data lead us to believe that this approach can be used to extract dephasing rates from experimental measurements of closed dots magnetoconductance with reasonable accuracy.

We now demonstrate the use of the above theory to extract dephasing times from the existing data points (mean values and error bars) of Folk et al. [11]. Fig. 2 presents these estimates as symbols and error bars, respectively, and

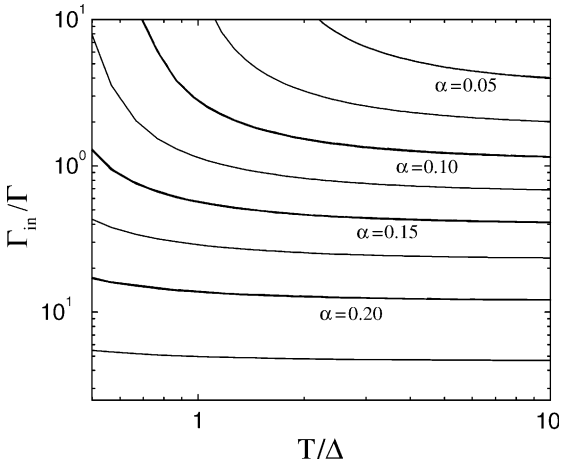

Fig. 3. A contour plot of α as a function of T/Δ and $\Gamma_{in}/\overline{\Gamma}$, based on the high temperature approximation. The values the bold contours are specified. Given T, Δ and α from future experiments, one can extract $\Gamma_{in}/\overline{\Gamma}$ from this figure (reproduced from [14]).

compares them with open dot values [6]. A clear enhancement of the dephasing times compared to open dots is observed. In addition, dephasing times strongly depend on Δ (as can be seen at $T = 45$ mK). This is in contrast to open dot results [6]. An additional suppression of α for $k_B T < \Delta$, resulting from level-spacing fluctuations was not included so-far but will be discussed in Section 5 [15]. Because of this effect, our results *underestimate* the dephasing times for $k_B T < \Delta$. Also note that, the result for the $\Delta = 0.9$ μeV quantum dot which is consistent with $\tau_\phi = 0$ should be interpreted carefully since the result implies $\hbar\Gamma_{\rm in} > \Delta$ and the master equation is not applicable anymore. Based on our analysis, the recent experiment [11], measuring dephasing in closed quantum dots is consistent with dephasing due to electron–electron interaction alone, including the prediction of the critical vanishing of dephasing rate. However, given the large error bars of the current experimental data, one cannot exclude an algebraic behavior or even a saturation of the dephasing rates for $T \to 0$. Nevertheless, the behavior is clearly different from that of open quantum dots [6] and is Δ-dependent.

Since the analytic form of our results, as detailed in Appendix A, is cumbersome, we provide Fig. 3, which can be used to practically analyze future experiments. The figure presents α as a contour-plot in the space spanned by $k_B T/\Delta$ and $\Gamma_{\rm in}/\overline{\Gamma}$. For a given measurement, with known temperature and α, one can easily read the proper value of $\Gamma_{\rm in}/\overline{\Gamma}$.

5. RMT eigenlevel fluctuations

In the previous sections we studied the effect of dephasing on the magnetoconductance of a closed quantum dot. Here we show that at low temperatures, where the dephasing mechanism is not very effective, another effect arises, due to the fluctuations in the RMT spectrum, that reduces α. However, very recently Usaj and Baranger [18] studied the effect of the exchange term and found that this term can actually increase α.

Previous works [4,10,12,14,17] have generally considered a picket-fence spectrum, i.e., a rigid level spacing between successive eigenlevels in the quantum dot, for the calculation of the conductance. This ignores the effect of spectral eigenlevel fluctuations. The picket-fence spectrum is a good approximation for both very high temperatures and very low temperatures [4], and a comparison of $P(G^{\max})$ with full RMT statistics and a picket-fence spectrum without spin-degeneracy at three temperatures showed only minor deviations [19].

Here, we study the full RMT statistics in detail with and without spin-degeneracy, and find significant differences compared to the picket-fence spectrum, in particular in an experimentally relevant regime $k_B T \lesssim \Delta$. The spectral fluctuations lead to lower values of α than 1/4 such that this value is not universal, even in the absence of any dephasing mechanism. One therefore has to be careful while using α as a probe for dephasing in this temperature regime.

Within the constant interaction model, the conductance of a quantum dot is given by the formula [16]

$$G = \frac{e^2}{kT} \sum_j \frac{\Gamma_i^{\rm L}\Gamma_i^{\rm R}}{\Gamma_i^{\rm L} + \Gamma_i^{\rm R}} P_{\rm eq}(N) P(E_i|N)[1 - f(E_i - \mu)]. \tag{25}$$

Without inelastic scattering Eq. (25) can be easily obtained from the solution of the master equation (19)

$$\Psi_{\mathcal{N}}(\{n_i\}) = \text{const} + \frac{1}{2} \sum_j \delta_{n_j 1} \frac{\Gamma_j^{\rm L} - \Gamma_j^{\rm R}}{\Gamma_j^{\rm L} + \Gamma_j^{\rm R}}.$$

Contrary to Section 4 we now employ the full RMT distribution of the eigenlevel energies E_i [4]. The first term in the sum $\Gamma_i^{\rm L}\Gamma_i^{\rm R}/(\Gamma_i^{\rm L} + \Gamma_i^{\rm R})$ depends only on the eigenfunctions of the dot, and thus is uncorrelated with the spectrum within the RMT approach. The ensemble average of this term in the absence (GOE) or presence (GUE) of a magnetic field is

$$\left\langle\left\langle \frac{\Gamma_i^{\rm L}\Gamma_i^{\rm R}}{\Gamma_i^{\rm L} + \Gamma_i^{\rm R}} \right\rangle\right\rangle = \begin{cases} 1/4, & \text{GOE}, \\ 1/3, & \text{GUE}. \end{cases} \tag{26}$$

This yields the value $\alpha = 1/4$ if the weights $P(E_i|N)$ are the same for both ensembles. This should be the case in the low temperature regime $k_B T \ll \Delta$ since only one level E_0 contributes with maximal weight, $P(E_i|N) \approx \delta_{i0}$. In general, the main contribution to the sum comes from $O(k_B T/\Delta)$ levels around the Fermi energy which gives the same contribution at large temperatures $k_B T \gg \Delta$ for the GOE and GUE, $\alpha = 1/4$ in this regime as well.

However, for $k_B T \lesssim \Delta$, the probability to have more than one level in an energy window $k_B T$ around the Fermi energy is increased for the RMT eigenlevel distribution compared to the picket-fence spectrum. These additional levels enhance the conductance. Since there are more close-by levels for the GOE case, due to the weaker level repulsion, the GOE conductance is enhanced more, and α is suppressed.

A second important effect is the optimization of the chemical potential for the Coulomb blockade peak. This effect was generally ignored, as it is technically cumbersome to consider, and is not significant for both very low and very high temperatures. Disregarding this effect means that a theorist optimized the chemical potential w.r.t. the averaged conductance, instead of optimizing for every realization as in the experiment. Whenever there is a close-by level, the position of the peak is shifted to optimize the contribution from both levels. Typically, a level with very low tunneling rates (and, thus, suppressed conductance peak) would get enhanced significantly by contributions from its neighbors. If the tunneling rate of a neighboring level is much higher, the peak position $\mu^{\max}$ is shifted towards it. As the distribution of level spacings is different depending on the existence of magnetic field, this enhancement mechanism is again more effective in the absence of magnetic field (GOE), where probabilities of small spacing and of small conductances are higher. Thus, this effect which was neglected in [19] suppresses α even further.

We evaluated the sum (25) numerically by drawing $\Gamma_i^{\mathrm{L(R)}}$ from the Porter-Thomas distribution and E_i according to the Wigner-Dyson distribution. Levels within a window of $\pm 4k_{\mathrm{B}}T$ around the Fermi energy have been taken into account and the Fermi energy μ in Eq. (25) has been adjusted to yield $G^{\max}$ for every realization.

Fig. 4 compares the probability distribution $P(G^{\max})$ for a picket-fence spectrum vs. the full RMT level statistics. As explained above, RMT spectral fluctuations enhance the conductance. In particular, the probability to have a very low

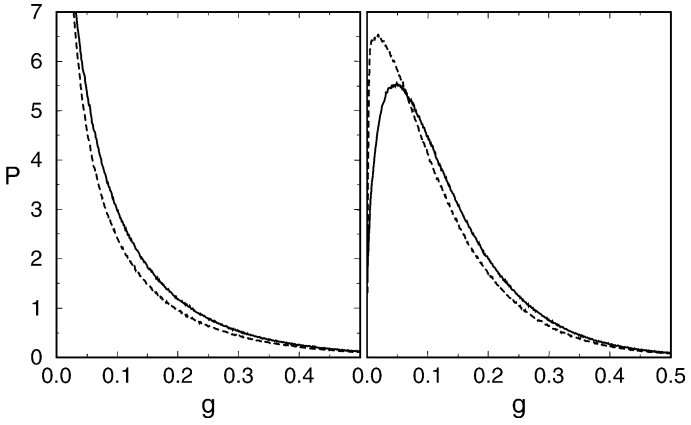

Fig. 4. Probability distribution $P(g)$ of the dimensionless closed dot conductance g defined by $G^{\max} = e^2/\hbar\,(\hbar\overline{\Gamma}/k_{\mathrm{B}}T)g$ at $k_{\mathrm{B}}T = 0.2\Delta$ in the presence of spin-degeneracy (left: GOE; right: GUE; solid line: RMT spectral fluctuations; dashed line: picket fence) (reproduced from [15]).

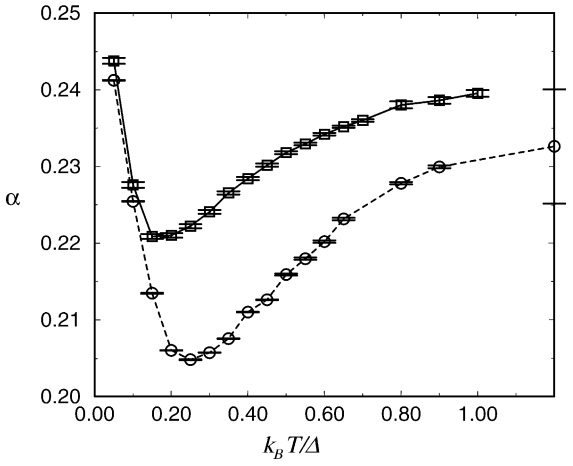

Fig. 5. Magnetoconductance α vs. $k_{\mathrm{B}}T/\Delta$ for the spin-degenerate case (dashed line) and without spin-degeneracy (solid line). Taking into account the RMT spectral fluctuations, α is reduced from its "universal" value $\alpha = 1/4$, in particular in the experimental relevant regime $0.1\Delta < k_{\mathrm{B}}T < 0.8\Delta$ (reproduced from [15]).

$G^{\max}$ is reduced and the probability to have an intermediate $G^{\max}$ is enhanced. The reason for the reduction is that a very low $G^{\max}$ requires Γ^{L} or Γ^{R} in Eq. (25) to be low. RMT spectral fluctuations enhance the contributions from close-by levels, which typically do not have a low value of $\Gamma^{\mathrm{L(R)}}$ at the same time. Thus, the peak position of μ is shifted towards a close-by level and the conductance occurs through both levels. Notably, the effect of phase-breaking inelastic scattering processes leads to similar changes (see Section 4) [14].

Deviations of α from the "universal" value 1/4 have been interpreted as being a result of dephasing. While dephasing would certainly suppress α, we note here that in the regime $k_{\mathrm{B}}T \lesssim \Delta$, the spectral fluctuation effects discussed above, lead to a similar effect. In Fig. 5 we present the results for α as a function of the scaled temperature $k_{\mathrm{B}}T/\Delta$, for both spin-degenerate spectrum and the case of broken symmetry. While the effect seems to be small, one should keep in mind that in the low temperature regime, even very strong dephasing does not suppress α substantially (see Fig. 1 and [12]), and thus the correction due to spectral fluctuations is comparable with or even larger than the effect of dephasing [12,14]. One should therefore cautiously use α as a probe of dephasing in this regime.

6. Conclusion

In conclusion, we provide a theoretical approach to extract the inelastic scattering rate in closed dots from experimental measurements of the weak-localization correction α. Analyzing a recent experiment by Folk et al. [11], we see a clear enhancement of the dephasing time compared with open dots values. Contrary to open quantum dots, the dephasing time is also dependent on the size of the quantum dot. These results agree with the theoretical predictions for electron–electron interaction, in particular, a vanishing dephasing rate at a critical *Δ-dependent* temperature. We note, however, that the available experimental data is limited and has considerably statistical uncertainties. Thus, future experiments are necessary and we offer Fig. 3 to extract the temperature and level-spacing dependence of the inelastic scattering rate and to thoroughly test the prediction of a diverging dephasing time.

When analyzing future experiments one should take into account that in the low temperature regime RMT spectral fluctuation and the exchange term [18] effect the magneto conductance α and probability distribution function $P(G^{\max})$, in particular in the regime $0.1\Delta < k_{\mathrm{B}}T < 0.8\Delta$. Even without dephasing α is different from 1/4 and temperature dependent; α can be reduced down to $\alpha \approx 0.2$ by RMT eigenlevel fluctuations, below the lower limit of a picket-fence model *with* dephasing (see Fig. 1) in this temperature range.

Acknowledgements

We are happy to acknowledge intensive and very helpful discussions with I.L. Aleiner, J.A. Folk, and C.M. Marcus. This work has been supported by ARO, DARPA, and the Alexander von Humboldt foundation.

Appendix A. Analytic expansion of Eq. (24)

In this appendix we show how to perform the disorder averaging in Eq. (24). For that purpose, let us rewrite this equation in the following way:

$$\langle G\rangle \sim \left\langle \sum_i \omega_i \left(\frac{\Gamma_i^{\mathrm{L}}\Gamma_i^{\mathrm{R}}}{\Gamma_i^{\mathrm{L}}+\Gamma_i^{\mathrm{R}}+\Gamma_{\mathrm{in}}^{*}} + \frac{\Gamma_i^{\mathrm{L}}\Gamma_{\mathrm{in}}^{*}}{\Gamma_i^{\mathrm{L}}+\Gamma_i^{\mathrm{R}}+\Gamma_{\mathrm{in}}^{*}} \frac{\sum_j \omega_j \Gamma_j^{\mathrm{R}}/(\Gamma_j^{\mathrm{L}}+\Gamma_j^{\mathrm{R}}+\Gamma_{\mathrm{in}}^{*})}{\sum_j \omega_j (\Gamma_j^{\mathrm{L}}+\Gamma_j^{\mathrm{R}})/(\Gamma_j^{\mathrm{L}}+\Gamma_j^{\mathrm{R}}+\Gamma_{\mathrm{in}}^{*})} \right) \right\rangle, \tag{A.1}$$

where $\omega_i \equiv f_i(1-f_i)$, and we omitted the irrelevant prefactors which do not change upon applying magnetic field.

Within RMT, both the eigenvalues and the eigenfunctions fluctuate. Since the statistical properties of the spectrum are uncorrelated with those of the eigenfunctions, one can separately average upon the Γ's and the ω's. Here, we restrict ourselves to the approximation of a *picket-fence* spectrum, in which the spectrum is assumed to be equally spaced, ignoring the RMT spectral fluctuations, such that one has to average upon the Γ's alone. The picket-fence approximation is reasonable for large enough temperatures.

Before we start the averaging, we introduce some definitions to simplify future notation. First, we define the sums

$$F_m \equiv \sum_j \omega_j^m \tag{A.2}$$

and the integrals

$$I_0 \equiv \left\langle \frac{\Gamma_1\Gamma_2}{\Gamma_1+\Gamma_2+\Gamma_{\rm in}^*} \right\rangle \tag{A.3}$$

$$= \int \mathrm{d}\Gamma_1\,\mathrm{d}\Gamma_2 \frac{\Gamma_1\Gamma_2}{\Gamma_1+\Gamma_2+\Gamma_{\rm in}^*} P_\beta(\Gamma_1)P_\beta(\Gamma_2), \tag{A.4}$$

$$I_{mn} \equiv \left\langle \frac{\Gamma_1^m\Gamma_2^n}{(\Gamma_1+\Gamma_2+\Gamma_{\rm in}^*)^{m+n}} \right\rangle, \tag{A.5}$$

where the average is for Γ_1 and Γ_2 being two independent random numbers distributed according to the Porter-Thomas distribution $P_\beta(\Gamma)$. These integrals depend on $\Gamma_{\rm in}^*$ and β, but we suppress this in the notation for simplicity. The analytical values of these integrals are given below.

In terms of these quantities, the first term in Eq. (A.1) is easily expressed, and one gets the contribution

$$\left\langle \sum_i \omega_i \frac{\Gamma_i^{\rm L}\Gamma_i^{\rm R}}{\Gamma_i^{\rm L}+\Gamma_i^{\rm R}+\Gamma_{\rm in}^*} \right\rangle = F_1 I_0. \tag{A.6}$$

However, the second term is more cumbersome, due to the appearance of the different Γ's in the denominator. In order to overcome this, we employ an expansion around the average. We use short notation for the Γ's fractions, defining

$$a_m \equiv \frac{\Gamma_m^{\rm L}}{\Gamma_m^{\rm L}+\Gamma_m^{\rm R}+\Gamma_{\rm in}^*}, \quad b_m \equiv \frac{\Gamma_m^{\rm R}}{\Gamma_m^{\rm L}+\Gamma_m^{\rm R}+\Gamma_{\rm in}^*} \tag{A.7}$$

and rewrite the denominator in the following way:

$$\sum_j \omega_j(a_j+b_j) = \sum_j \omega_j(2I_{10}+(a_j-I_{10})+(b_j-I_{10})) \tag{A.8}$$

$$= 2F_1I_{10}\left(1+\frac{\sum_k \omega_k((a_k-I_{10})+(b_k-I_{10}))}{2F_1I_{10}}\right). \tag{A.9}$$

Using this form, one can write the second term of Eq. (A.1) in the following way:

$$\left\langle \frac{\Gamma_{\rm in}^*(\sum_i \omega_i a_i)(\sum_j \omega_j b_j)}{2F_1I_{10}} \sum_{m=0}^{\infty}(-1)^m\left(\frac{\sum_k \omega_k(a_k+b_k-2I_{10})}{2F_1I_{10}}\right)^m \right\rangle. \tag{A.10}$$

One can now average term by term the infinite sum over m. As we focus in the high-T limit, we will collect the terms according to their T dependence. For that purpose, one has to bear in mind that the T-dependence comes from the F_m's. Asymptotically (for large T) they are all linear in T, and can be approximated by

$$F_1 \approx T, \quad F_2 \approx T/6, \quad F_3 \approx T/30\ldots \tag{A.11}$$

Thus we would like to collect terms in powers of the F_m's. It is important to notice that the expression summed over k has vanishing average. Therefore, the only occasion in which it contributes is when the summation index is "paired" with some other index. Such pairing reduced the number of contributing terms, and thus the power of T. A term with no pairing contributes to the leading order (i.e., $\mathrm{O}(k_{\rm B}T/\Delta)$), a term with one pair contributes to the next order (i.e., $\mathrm{O}(1)$), etc. This is why the expansion converges, taking large enough m, as will be explained below.

The first term in the sum, $m=0$, results in the following contribution:

$$\frac{\Gamma_{\rm in}^*}{2F_1I_{10}}\left\langle \sum_i \omega_i a_i \sum_j \omega_j b_j \right\rangle = \frac{\Gamma_{\rm in}^*}{2F_1}(I_{10}(F_1^2-F_2)+I_{11}F_2) \tag{A.12}$$

and one already sees that it gives both terms $\mathrm{O}(\Delta/k_{\rm B}T)$ and terms $\mathrm{O}(1)$.

For the moment m, there are m such terms needed to be paired, and the minimal way to do it is to create $m/2$ pairs. This is the reason why it is sufficient to consider a finite number of moments for a certain power of T. The first moment $m=1$ is given by

$$-\frac{\Gamma_{\rm in}^*}{(2F_1I_{10})^2}\left\langle \sum_i \omega_i a_i \sum_j \omega_j b_j \sum_k \omega_k(a_k+b_k-2I_{10}) \right\rangle \tag{A.13}$$

and contributes only for $k = i$ or $k = j$. Collecting all terms, the contribution of this term is

$$-\frac{\Gamma^*_{\rm in}F_2}{4F_1I_{10}}(I_{20}+I_{11}-2I_{10}^2)-\frac{\Gamma^*_{\rm in}F_3}{2F_1^2I_{10}^2}(I_{21}-I_{10}(I_{20}+2I_{11}-2I_{10}^2)) \tag{A.14}$$

For the next moments, the number of possible pairings is big. Here we aim at calculating the first three terms only, i.e., up to $O(\Delta/k_BT)$, and thus we allow only two pairings per term. For $m = 2$ the term to be averaged is

$$-\frac{\Gamma^*_{\rm in}}{(2F_1I_{10})^3}\left\langle\sum_i\omega_ia_i\sum_j\omega_jb_j\sum_{k1}\omega_{k_1}(a_{k_1}+b_{k_1}-2I_{10})\sum_{k2}\omega_{k_2}(a_{k_2}+b_{k_2}-2I_{10})\right\rangle \tag{A.15}$$

and the contributing pairings are (a) $k_1 = k_2$ (one pairing) (b) $k_1 = i$, $k_2 = j$ and vice-versa. The resulting contributions (ignoring terms $O(\Delta/k_BT)$) are

$$\text{(a)}\ \frac{\Gamma^*_{\rm in}F_2}{4F_1I_{10}}(I_{20}+I_{11}-2I_{10}^2)+\frac{\Gamma^*_{\rm in}F_3}{4F_1^2I_{10}^2}(3I_{21}+I_{30}-2I_{10}(3I_{20}+3I_{11}-4I_{10}^2)), \tag{A.16}$$

$$\text{(b)}\ \frac{\Gamma^*_{\rm in}F_2^2}{4F_1^3I_{10}^3}(I_{20}+I_{11}-2I_{10}^2)^2. \tag{A.17}$$

The third moment, $m = 3$, also has two contributions (a) $k1 = k2 = k3$ and (b) $k1 = i$, $k2 = k3$ (and permutations). The resulting $O(1/T)$ contributions are

$$\text{(a)}\ -\frac{\Gamma^*_{\rm in}F_3}{8F_1^2I_{10}^2}(I_{30}+3I_{21}-6I_{10}(I_{11}+I_{20})+8I_{10}^3), \tag{A.18}$$

$$\text{(b)}\ -\frac{3\Gamma^*_{\rm in}F_2^2}{4F_1^3I_{10}^3}(I_{20}+I_{11}-2I_{10}^2)^2. \tag{A.19}$$

The fourth moment $m = 4$ gives a $O(1/T)$ contribution only for the pairing $m1 = m2$, $m3 = m4$ (and permutations), leading to

$$\frac{3\Gamma^*_{\rm in}F_2^2}{8F_1^3I_{10}^3}(I_{20}+I_{11}-2I_{10}^2)^2. \tag{A.20}$$

For the fifth moment to contribute, at least three pairings are needed, and thus its leading order contribution is $O(1/T^2)$. Similarly, one can easily verify that higher moments do not contribute to $O(1/T)$.

Collecting all the contributions from Eqs. (A.6), (A.12), (A.14) and (A.16)–(A.20), one obtains the final expression for $\langle G\rangle$:

$$\langle G\rangle \sim F_1(I_0+\Gamma^*_{\rm in}I_{10}/2)+\frac{\Gamma^*_{\rm in}F_2}{2F_1}\frac{I_{11}-I_{20}}{2I_{10}}+\frac{\Gamma^*_{\rm in}F_3}{8F_1^2}\frac{I_{30}-I_{21}+2I_{10}(I_{11}-I_{20})}{8I_{10}^2}-\frac{\Gamma^*_{\rm in}F_2^2}{8F_1^3}\frac{(I_{20}+I_{11}-2I_{10}^2)^2}{I_{10}^3}$$
$$+O([\Delta/k_BT]^{-2}). \tag{A.21}$$

In order to obtain the magnetoconductance, one needs to have the values of the integral I_{mn} for the *GOE* ($\beta = 1$) and *GUE* ($\beta = 2$) cases. These can be directly computed and the results are

$$I_0=\begin{cases}\frac{1}{4}-\frac{\Gamma^*_{\rm in}}{8}+\frac{(\Gamma^*_{\rm in})^2}{16}\exp(\Gamma^*_{\rm in}/2)Ei(1,\Gamma^*_{\rm in}/2), & \text{GOE},\\ \frac{1}{3}-\frac{\Gamma^*_{\rm in}}{6}+\frac{(\Gamma^*_{\rm in})^2}{6}-\frac{(\Gamma^*_{\rm in})^3}{6}\exp(\Gamma^*_{\rm in})Ei(1,\Gamma^*_{\rm in}), & \text{GUE},\end{cases} \tag{A.22}$$

$$I_{10}=\begin{cases}\frac{1}{2}-\frac{\Gamma^*_{\rm in}}{4}\exp(\Gamma^*_{\rm in}/2)Ei(1,\Gamma^*_{\rm in}/2), & \text{GOE},\\ \frac{1}{2}-\frac{\Gamma^*_{\rm in}}{2}+\frac{(\Gamma^*_{\rm in})^2}{2}\exp(\Gamma^*_{\rm in})Ei(1,\Gamma^*_{\rm in}), & \text{GUE},\end{cases} \tag{A.23}$$

$$I_{20}=\begin{cases}\frac{3}{8}+\frac{3\Gamma^*_{\rm in}}{16}-\left(\frac{3\Gamma^*_{\rm in}}{8}+\frac{3(\Gamma^*_{\rm in})^2}{32}\right)\exp(\Gamma^*_{\rm in}/2)Ei(1,\Gamma^*_{\rm in}/2), & \text{GOE},\\ \frac{1}{3}-\frac{2\Gamma^*_{\rm in}}{3}-\frac{(\Gamma^*_{\rm in})^2}{3}+\left((\Gamma^*_{\rm in})^2+\frac{(\Gamma^*_{\rm in})^3}{3}\right)\exp(\Gamma^*_{\rm in})Ei(1,\Gamma^*_{\rm in}), & \text{GUE},\end{cases} \tag{A.24}$$

$$I_{11}=\begin{cases}I_{20}/3, & \text{GOE},\\ I_{20}/2, & \text{GUE},\end{cases} \tag{A.25}$$

$$I_{30} = \begin{cases} \frac{5}{16} + \frac{25\Gamma^*_{\rm in}}{64} + \frac{5(\Gamma^*_{\rm in})^2}{128} - \left(\frac{15\Gamma^*_{\rm in}}{32} + \frac{15(\Gamma^*_{\rm in})^2}{64} + \frac{5(\Gamma^*_{\rm in})^3}{256}\right) \exp(\Gamma^*_{\rm in}/2) Ei(1, \Gamma^*_{\rm in}/2), & \text{GOE}, \\ \frac{1}{4} - \frac{3\Gamma^*_{\rm in}}{4} - \frac{7(\Gamma^*_{\rm in})^2}{8} - \frac{(\Gamma^*_{\rm in})^3}{8} + \left(\frac{3(\Gamma^*_{\rm in})^2}{2} + (\Gamma^*_{\rm in})^3 + \frac{(\Gamma^*_{\rm in})^4}{8}\right) \exp(\Gamma^*_{\rm in}) Ei(1, \Gamma^*_{\rm in}), & \text{GUE}, \end{cases} \tag{A.26}$$

$$I_{21} = \begin{cases} I_{30}/5, & \text{GOE}, \\ I_{30}/3, & \text{GUE}, \end{cases} \tag{A.27}$$

where $Ei(1,x)$ is the exponential-integral function

$$Ei(1,x) = \int_{t=1}^{\infty} \frac{\mathrm{e}^{-xt}\,\mathrm{d}t}{t}. \tag{A.28}$$

We thus obtained a closed expression for the conductance for the GOE and GUE cases. Using this, one can evaluate α in the high temperature regime.

References

[1] Altshuler BL, Gefen Y, Kamenev A, Levitov LS. Phys Rev Lett 1997;78:2803.
[2] See, e.g., Rivas AMF, Mucciolo ER, Kamenev A. Phys Rev B 2002;65:155309, and references therein.
[3] Aleiner IL, Brouwer PW, Glazman LI. Phys Rep 2002;358:309.
[4] Alhassid Y. Rev Mod Phys 2000;72:895.
[5] Chang AM, Baranger HU, Pfeiffer LN, West KW, Chang TY. Phys Rev Lett 1996;76:1695;
Folk JA, Patel SR, Godijn SF, Huibers AG, Cronenwett SM, Marcus CM, Campman K, Gossard AC. Phys Rev Lett 1996;76:1699.
[6] Huibers AG, Switkes M, Marcus CM, Campman K, Gossard AC. Phys Rev Lett 1998;81:200;
Huibers AG, Folk JA, Patel SR, Marcus CM, Duruöz CI, Harris Jr JS. Phys Rev Lett 1999;83:5090.
[7] Clarke RM, Chan IH, Marcus CM, Duruöz CI, Harris Jr JS, Campman K, Gossard AC. Phys Rev B 1995;52:2656.
[8] See Sivan U, Milliken FP, Milkove K, Rishton S, Lee Y, Hong JM, Boegli V, Kern D, DeFranza M. Europhys Lett 1994;25:605 and references therein.
[9] Patel SR, Stewart DR, Marcus CM, Gökçedağ M, Alhassid Y, Stone AD, Duruöz CI, Harris Jr JS. Phys Rev Lett 1998;81:5900.
[10] Alhassid Y, Gökçedağ M, Stone AD. Phys Rev B 1998;58:R7524.
[11] Folk JA, Patel SR, Marcus CM, Duruöz CI, Harris JS. Phys Rev Lett 2001;87:206802.
[12] Beenakker CWJ, Schomerus H, Silvestrov PG. Phys Rev B 2001;64:033307.
[13] Rupp T, Alhassid Y, Malhotra S. cond-mat/0201055.
[14] Eisenberg E, Held K, Altshuler BL. Phys Rev Lett 2002;88:136801.
[15] Held K, Eisenberg E, Altshuler BL. cond-mat/0202098.
[16] Beenakker CWJ. Phys Rev B 1991;44:1646.
[17] Jalabert A, Stone AD, Alhassid Y. Phys Rev Lett 1992;68:3468.
[18] Usaj G, Baranger HU. private communication.
[19] Alhassid Y, Gökçedağ M, Stone AD. Phys Rev B 1998;58:7524.